Research Article

Significance of p53-Binding Protein 1 Nuclear Foci in Cervical Squamous Intraepithelial Lesions: Association With High-Risk Human Papillomavirus Infection and P16^{INK4a} Expression

Sayaka Kawashita, MD[1], Katsuya Matsuda, PhD[2], Hisayoshi Kondo, PhD[3], Yuriko Kitajima, PhD[1], Yuri Hasegawa, PhD[1], Takako Shimada, PhD[1], Michio Kitajima, PhD[1], Kiyonori Miura, PhD[1], Masahiro Nakashima, PhD[2], and Hideaki Masuzaki, PhD[1]

Abstract

As p53-binding protein 1 (53BP1) localizes to the sites of DNA double-strand breaks and rapidly forms nuclear foci (NF), and its presence may be an indicator of endogenous genomic instability (GIN). We previously showed that 53BP1 NF in cervical cells increase with neoplastic progression, indicating the significance of 53BP1 expression for the estimation of malignant potential during cervical carcinogenesis. This study aimed to further elucidate the impact of 53BP1 expression as a biomarker for cervical squamous intraepithelial lesion (SIL). A total of 81 tissue samples, including 17 of normal cervical epithelium, 22 of cervical intraepithelial neoplasia (CIN) 1, 21 of CIN2, and 21 of CIN3, from patients positive for high-risk human papillomavirus (HR-HPV) were used for double-label immunofluorescence of 53BP1 and Ki-67/p16^{INK4a} expression and HR-HPV in situ hybridization. We analyzed associations between 53BP1 expression type with parameters such as CIN grade, HR-HPV infection status, p16^{INK4a} expression, and CIN prognosis. Expression type of 53BP1 was significantly associated with histological grade of CIN and HR-HPV in situ hybridization signal pattern ($P < .0001$). There was a significant correlation between 53BP1 and p16^{INK4a} expression levels ($r = .73$, $P < .0001$). However, there was no association between 53BP1 expression type and CIN prognosis. We propose that 53BP1 expression type is a valuable biomarker for SIL, which can help estimate the grade and GIN of cervical lesions reflecting replication stress caused by the integration of HR-HPV to the host genome.

Keywords

cervical squamous intraepithelial lesion, 53BP1, genomic instability, high-risk human papillomavirus, p16^{INK4a}

Introduction

The p53-binding protein 1 (53BP1), belonging to the family of evolutionarily conserved DNA damage response (DDR) proteins, rapidly localizes at the sites of DNA double-strand breaks[1,2] to activate nonhomologous end-joining repair machinery by working with other DDR molecules.[3-6] Genomic instability (GIN), considered as an important hallmark of malignant tumors, is occasionally evident in the precancerous stage during carcinogenesis. Given that induction of

[1] Department of Obstetrics and Gynecology, Nagasaki University Graduate School of Biomedical Sciences, Nagasaki, Japan
[2] Department of Tumor and Diagnostic Pathology, Atomic Bomb Disease Institute, Nagasaki University, Nagasaki, Japan
[3] Biostatistics Section, Division of Scientific Data Registry, Atomic Bomb Disease Institute, Nagasaki University, Nagasaki, Japan

Corresponding Author:
Masahiro Nakashima, Department of Tumor and Diagnostic Pathology, Atomic Bomb Disease Institute, Nagasaki University, 1-12-4 Sakamoto, Nagasaki 852-8523, Japan.
Email: moemoe@nagasaki-u.ac.jp

Creative Commons Non Commercial CC BY-NC: This article is distributed under the terms of the Creative Commons Attribution-NonCommercial 4.0 License (https://creativecommons.org/licenses/by-nc/4.0/) which permits non-commercial use, reproduction and distribution of the work without further permission provided the original work is attributed as specified on the SAGE and Open Access pages (https://us.sagepub.com/en-us/nam/open-access-at-sage).

endogenous DDR is a characteristic manifestation of GIN, we propose that 53BP1 expression can be a useful tool to estimate the level of GIN as well as the malignant potential of human tumors. Indeed, we have previously demonstrated that the presence of 53BP1 nuclear foci (NF) by the immunofluorescence method can serve as a valuable molecular marker for GIN during carcinogenesis in thyroid and skin.[7,8]

Development of uterine cervical cancer is a multistep process. It is also well established that persistent infections with high-risk human papillomavirus (HR-HPV) cause high-grade premalignant lesions and subsequent invasive cancer of the uterine cervix. [9-12] We have previously demonstrated that the number of 53BP1 NF in cervical cells appeared to increase with cancer progression.[13] The distribution of 53BP1 NF was similar to that of punctate HPV signals as determined by in situ hybridization (ISH) and also to the pattern of $p16^{INK4a}$ overexpression, an established surrogate marker for HPV infection in cervical squamous intraepithelial lesion (SIL). Thus, 53BP1 NF are associated with viral infection and replication stress, and the immunofluorescence analysis of 53BP1 expression can be a useful tool to estimate GIN level during cervical carcinogenesis. However, our previous report[13] had limited information about some clinical parameters. There was insufficient information about the results of the HPV polymerase chain reaction (PCR) test, which is currently widely used. Moreover, the comparison between 53BP1 and $p16^{INK4a}$ was not objective and practical. To further elucidate the impact of 53BP1 expression as a biomarker for cervical carcinogenesis, we analyzed the relationships between the type of 53BP1 expression and parameters such as histological type of SIL, HR-HPV infection status by ISH, $p16^{INK4a}$ overexpression, and prognosis by utilizing the SIL cases in which HR-HPV infection was confirmed by PCR and for which a long-term prognosis was available.

Materials and Methods

Cervical Tissue Samples

A total of 81 archival uterine cervical biopsy samples from patients with abnormal cytology were used. Because all samples used in this study were obtained from 2007 to 2010, cervical SILs were classified according to the third World Health Organization Classification of Tumors of the Breast and Female Genital Organs (2004).[14] The pathological diagnosis was confirmed by more than 2 certified pathologists. Clinicopathological profiles of these patients are summarized in Table 1. Histologically, our samples included 17 cases of normal cervical epithelium found in resected uterine biopsy samples, 22 cases of cervical intraepithelial neoplasia (CIN)1, 21 cases of CIN2, and 21 cases of CIN3. All samples were formalin-fixed, and paraffin-embedded tissues were prepared for immunofluorescence and ISH studies. For research purposes, all patients who consulted our institution underwent HPV genotyping test using hybrid capture methods at that time. To unify their HPV infection profiles, we selected patients who were certified positive for at least 1 of the 13 HR-HPVs (16, 18, 31, 33, 35, 39, 45, 51, 52, 56, 58, 59, or 68).

This study was retrospectively conducted in accordance with the tenets of the Declaration of Helsinki and approved by the institutional Ethical Committee for Medical Research at the Nagasaki University (approval date: July 24, 2015; #1506265). Following the guidelines of the Ethical Committee's official informed consent and disclosure system, detailed information regarding the study was available on our website (http://www-sdc.med.nagasaki-u.ac.jp/pathology/research/index.html). Patients were able to opt out of the study by following the instructions on the faculty website. All samples were selected from the archives of the Department of Obstetrics and Gynecology, Nagasaki University Hospital, between 2007 and 2010.

Table 1. Clinicopathological Profiles of the Patients in This Study.

| Clinicopathological Profiles	Normal	CIN1	CIN2	CIN3	P Value
n	17	22	21	21	
Age at diagnosis, years[a]	37.3 ± 11.0	36.3 ± 10.2	39.8 ± 12.7	41.1 ± 12.3	.53[b]
BMI, kg/m²[a]	21.4 ± 2.8	21.3 ± 2.7	21.8 ± 3.3	21.1 ± 2.6	.68[b]
Nulliparous/parous	8/9	13/9	9/12	11/10	.95[c]
Smokers	3	4	3	3	.70[c]
Usage of oral contraceptives	1	1	2	3	.27[c]
Type of HPV ISH signal, %					
Negative	NE	14 (63.6)	10 (47.6)	0	<.0001[d]
Diffuse		1 (4.5)	0	0	
Mixed		2 (9.0)	5 (23.8)	4 (19.0)	
Punctate		5 (22.7)	6 (28.6)	17 (81.0)	

Abbreviations: CIN, cervical intraepithelial neoplasia; BMI, body mass index; HPV, human papillomavirus; ISH, in situ hybridization; NE, not examined.
[a]Data are shown as mean ± standard deviation.
[b]Kruskal-Wallis test.
[c]Cochran-Armitage test.
[d]Jonckheere-Terpstra test.
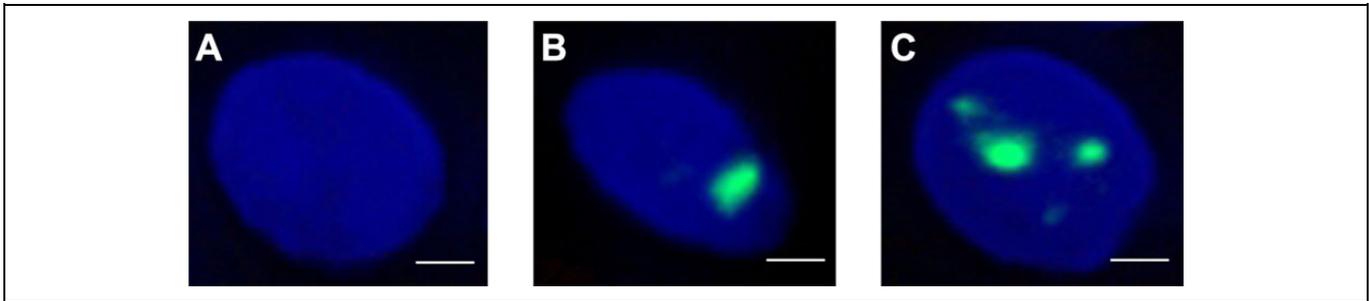
Figure 1. Three types of p53-binding protein 1 (53BP1) expression. A, Stable type—faint and diffuse nuclear staining. B, Low DNA damage response (DDR) type—1 or 2 discrete nuclear foci. C, High DDR type—3 or more discrete nuclear foci. Scale bar is 5 μm in all images.

Immunofluorescence Analysis of 53BP1 Expression

After antigen retrieval with microwave treatment in Dako REAL Target Retrieval Solution (Dako-Agilent technologies, Santa Clara, California), deparaffinized sections were preincubated with 10% normal goat serum. Tissue sections were then reacted with an anti-53BP1 rabbit polyclonal antibody (Bethyl Laboratories, Montgomery, Texas) at a 1:1000 dilution. The slides were subsequently incubated with Alexa Fluor 488-conjugated goat antirabbit antibody (Molecular Probes Inc, Eugene, Oregon). Specimens were counterstained with 4′,6-diamidino-2′-phenylindole dihydrochloride (DAPI; Vysis, Downers Grove, IL, USA) and photographed at 1000× magnification with a High Standard All-in-one Fluorescence Microscope (BIOREVO BZ-X700; KEYENCE Japan, Osaka, Japan). All 53BP1 expression signals were measured using image analysis software provided with the BIOREVO BZ-X700 microscope. The pattern of 53BP1 immunoreactivity was classified into 3 types as shown in Figure 1: (1) stable type—with faint nuclear staining; (2) low DDR type—with 1 or 2 discrete NF; and (3) high DDR type—with 3 or more discrete NF. The percentage of epithelial cells expressing each type of 53BP1 immunoreactivity was calculated in 5 consecutive fields along the basement membrane of each cervical lesion.

Double-Label Immunofluorescence Staining for 53BP1 and Ki-67/p16^{INK4a} Expression

For double staining, tissues were incubated with a mixture of rabbit polyclonal anti-53BP1(Bethyl Laboratories), mouse monoclonal anti-Ki-67 antibodies (MIB-1; DakoCytomation, Glostrup, Denmark), and diluted 1:100/mouse monoclonal anti-p16^{INK4a} antibodies (clone E6H4 in CINtec Histology Kit; Roche, Tucson, Arizona) and subsequently incubated with a mixture of Alexa Fluor 488-conjugated goat antirabbit and Alexa Fluor 594F (ab')-conjugated goat anti-mouse antibodies (Molecular Probes Inc). Specimens were counterstained with DAPI (Vysis) and photographed with a BIOREVO BZ-X700 microscope.

Detection of HR-HPV by ISH

In Situ Hybridization was performed with a GenPoint Tyramide signal amplification system (Dako-Agilent technologies) for HR-HPV (types 16, 18, 31, 33, 35, 39, 45, 51, 52, 56, 58, 59, and 68) according to the manufacturer's protocol. After deparaffinization and rehydration, the sections underwent microwave treatment in Dako REAL Target Retrieval Solution (Dako-Agilent technologies) for 20 minutes at 97°C. Sections were immersed in proteinase K (10 000×) for 10 minutes. After that, the sections were denatured at 90°C for 5 minutes and hybridized at 37°C overnight. Detection of the hybridized probe was performed with primary peroxidase-conjugated streptavidin, biotinyl tyramide, and secondary peroxidase-conjugated streptavidin. We used an anti-HRP mouse monoclonal antibody (Novus Biologicals, Littleton, Colorado) at a 1:1000 dilution and subsequently incubated samples with Alexa Fluor 594F (ab')-conjugated goat anti-mouse antibodies. Specimens were counterstained with DAPI (Vysis) and analyzed using a BIOREVO BZ-X700 microscope. High-risk-HPV ISH signals were evaluated according to the criteria described previously.[15-17] In brief, the patterns were as follows: (1) a diffuse pattern representing episomal HPV that correlated with viral replication; (2) a punctate pattern consisting of 1 or several discrete signals in the nucleus, indicating HPV integration into the genome; and (3) a mixed pattern with some areas containing only integrated or episomal copies and other areas where the integrated virus was hidden in episomal HPV copies.

Statistical Analysis

The Kruskal-Wallis test and Cochran-Armitage test were used to assess clinicopathological profiles of patients in this study. The Jonckheere-Terpstra test was used to assess associations between the histological type of CIN (normal, CIN1, CIN2, CIN3) and 53BP1 expression type (stable, low DDR, and high DDR) and between the status of HPV integration and 53BP1 expression type. The Cochran-Armitage test was used to assess the association between histological type of CIN and co-expression of DDR types and Ki-67. Fisher exact test was used to assess the associations between the status of HPV integration and co-expression of DDR types and Ki-67. Pearson correlation analysis was used to assess the correlation between 53BP1 and p16^{INK4a} expression levels. The Mann-Whitney U test and χ^2 test were used for univariate analysis of prognosis. Logistic regression was used for multivariate analysis of prognosis. Statistical analysis was performed with SAS 8.2 software

Table 2. Types of p53-Binding Protein 1 (53BP1) Expression Detected by Immunofluorescence.

CIN Grade	n	Counted Nuclei	Type of 53BP1 Expression, %			Co-Expression of DDR Types and Ki-67, %
			Stable	Low DDR	High DDR	
Normal	17	9188	83.8	13.5	2.7	0.6
CIN1	22	11 834	68.3	19.1	12.5	3.0
CIN2	21	11 251	67.9	19.8	12.3	2.9
CIN3	21	12 418	53.9	21.6	24.4	5.4
P value			<.0001[a]			<.0001[b]

Abbreviations: CIN, cervical intraepithelial neoplasia; DDR, DNA damage response.
[a]Jonckheere-Terpstra test.
[b]Cochran-Armitage test.

(SAS Institute, Cary, North Carolina) and GraphPad Prism 7 (GraphPad Software, San Diego, California). All statistical tests were 2-tailed and conducted with a significance level of $\alpha = .05$ ($P < .05$).

Results

Expression of 53BP1

The results of the immunofluorescence analyses for 53BP1 expression in CIN are presented in Table 2, and a representative image is depicted in Figure 2. In normal epithelium, 83.8% of nuclei showed the stable type of expression, and only 16.2% of nuclei showed DDR types. In CIN3, 53.9% of nuclei showed the stable type of expression and 46.0% of nuclei showed DDR types, including 24.4% showing high DDR type expression. Histological type of CIN was significantly associated with 53BP1 expression type ($P < .0001$). Then, we focused on the ratio of nuclei with high DDR type as an indicator to distinguish the CIN from normal epithelium and examined the receiver operating characteristic curve for the ratio of nuclei with
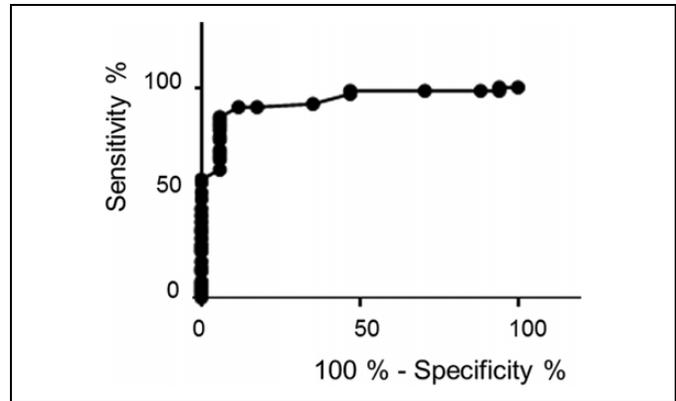
Figure 3. Receiver operating characteristic curve for detecting cervical squamous intraepithelial lesions (SILs). The area under the curve was 0.934 (95% confidence interval: 0.875-0.994). The cutoff index of the ratio of nuclei with high DNA damage response to distinguish SILs from normal epithelium was 6.35%. The sensitivity and specificity were 85.9% and 94.1%, respectively.

high DDR type (Figure 3). The area under the curve value was 0.934 (95% confidence interval, 0.875-0.994), suggesting reliable detection of CIN. If 6.35% was adopted as a cutoff value to diagnose CIN, the sensitivity and specificity were 85.9% and 94.1%, respectively.

Co-Expression of DDR Types and Ki-67

Double-label immunofluorescence for 53BP1 and Ki-67 expression was carried out to clarify the presence of abnormal DDR in CIN. We considered the colocalization of 53BP1 NF and Ki-67 expression in the nucleus as an abnormal DDR phenotype because DDR is normally activated during cell cycle arrest.[18-21] The frequency of co-expression of 53BP1 NF and Ki-67 in each cervical lesion is shown in Table 2. A significant positive association between the frequency of co-expression of 53BP1 NF and Ki-67 and histological type of CIN was observed ($P < .0001$).
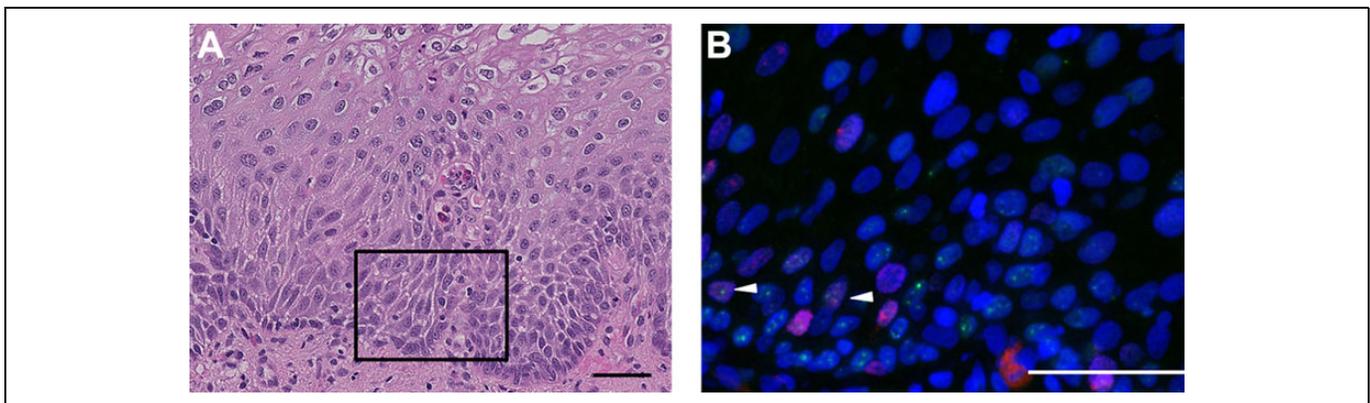
Figure 2. A case of squamous intraepithelial lesion with double-label immunofluorescence for p53-binding protein 1 (53BP1; green) and Ki-67 (red). A, Hematoxylin and eosin staining. B, Double-label immunofluorescence for 53BP1 and Ki-67 (magnification of A). Scale bar is 50 μm. There were several 53BP1 nuclear foci coexisting with Ki-67 nuclear staining (arrowhead) suggesting abnormal cell cycle regulation.

Table 3. Association Between Types of HPV ISH Signal and p53-Binding Protein 1 (53BP1) Expression.[a]

Type of HPV ISH signal	n	Counted Nuclei	Type of 53BP1 Expression, %			Co-expression of DDR Types and Ki-67, %
			Stable	Low DDR	High DDR	
Nonintegrated	25	12 507	71.8	17.0	11.2	2.69
Integrated	39	22 965	58.8	22.0	19.2	4.15
P value				<.0001[b]		<.0001[c]

Abbreviations: HPV, human papillomavirus; ISH, in situ hybridization; DDR, DNA damage response.

[a]Nonintegrated, negative and diffuse type; integrated, mixed and punctate types in Table 1.

[b]Jonckheere-Terpstra test.

[c]Fisher's exact test.

Association Between HR-HPV ISH Signal Types and 53BP1 Expression

The detection rates of HR-HPV DNA by ISH were 36.4%, 52.4%, and 100% in CIN1, CIN2, and CIN3, respectively, which were concordant with previous reports.[16] As shown in Table 1, the incidence of mixed and punctate types of ISH signal, which indicates integration of HPV genome into the host genome, was directly proportional to CIN grade ($P < .0001$). Furthermore, as shown in Table 3, incidences of both DDR types of 53BP1 expression and co-expression of DDR types and Ki-67 were significantly higher in CIN cases showing integrated (mixed and punctate) ISH signals. High-risk-HPV ISH signal type was significantly associated with 53BP1 expression pattern in CIN ($P < .0001$).

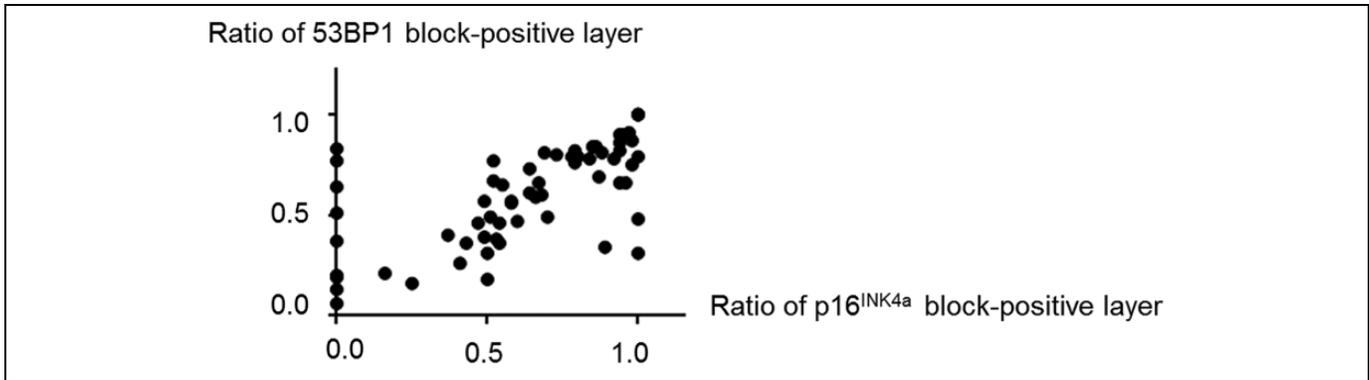## Correlation Between 53BP1 and p16^{INK4a} Expression Patterns

The value of p16^{INK4a} as a surrogate marker for the proliferative stress caused by HPV infection has been well established in SIL.[22,23] We carried out double-label immunofluorescence staining for 53BP1 and p16^{INK4a} to clarify the association between 53BP1 expression and the proliferative stress caused by HPV infection (Figure 4). Figure 5 shows a diagram of the correlation between the ratios of 53BP1 and p16^{INK4a} block-positive layer from the basal side of each CIN lesion. Negative p16^{INK4a} staining was observed in 5 cases of CIN1 (22.7%) and 5 cases of CIN2 (23.8%), whereas 53BP1 NF were observed in all cases. A significant correlation between 53BP1 and p16^{INK4a} expression levels ($r = 0.73$, $P < .0001$) was observed among the 54 cases of CIN with p16^{INK4a} immunoreactivity.

Association Between 53BP1 Expression and Prognosis of CIN

Association between 53BP1 expression type in CIN at the first diagnosis and its prognosis is summarized in Table 4. We
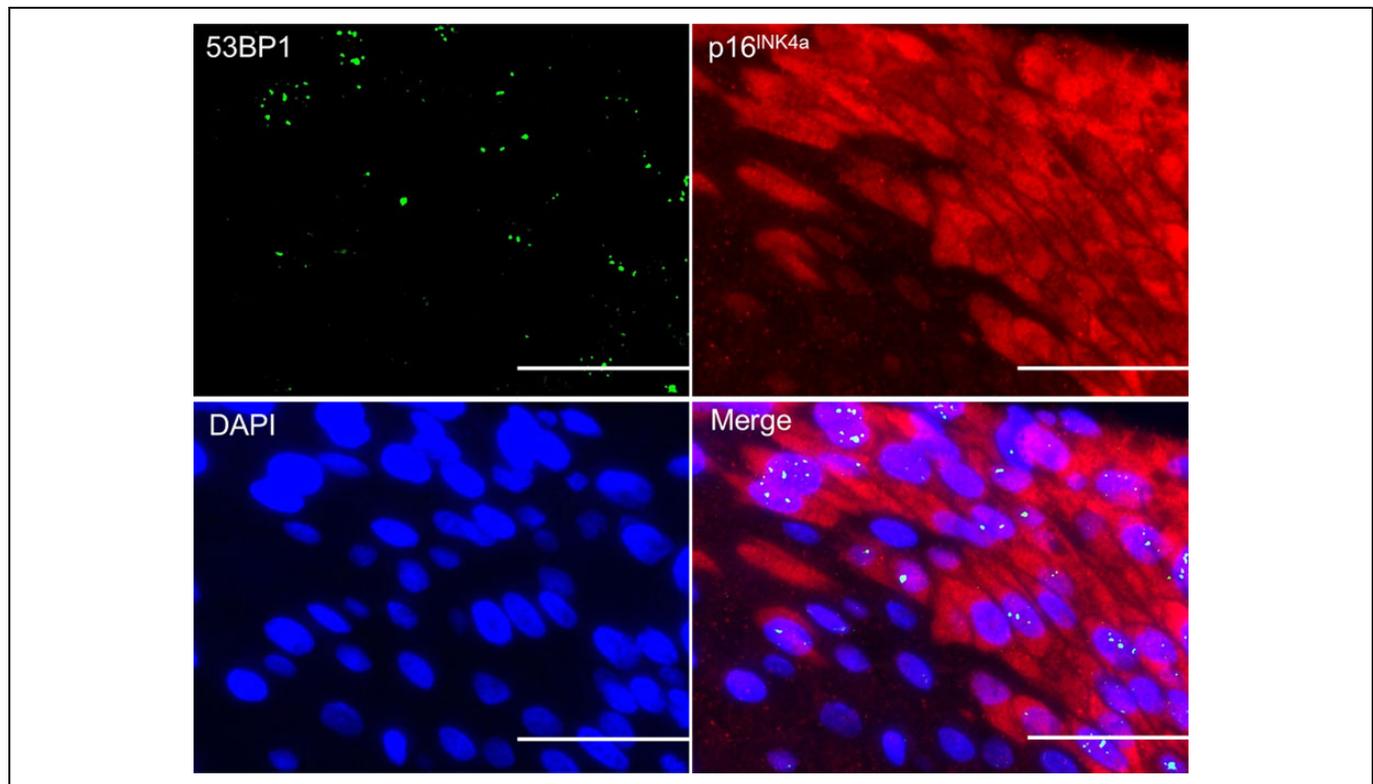
Figure 4. A case of squamous intraepithelial lesion with double-label immunofluorescence for p53-binding protein 1 (53BP1; green) and p16^{INK4a} (red). Scale bar is 50 μm. The distribution of 53BP1 nuclear foci was similar to that of p16^{INK4a}.

Figure 5. Comparison of p53-binding protein 1 (53BP1) and p16[INK4a] expression levels. In squamous intraepithelial lesions (SILs), positive for p16[INK4a], there was a significant correlation between 53BP1 and p16[INK4a] expression levels ($r = .73$, $P < .0001$). In p16[INK4a]-negative lesions, 53BP1 may be a superior test to distinguish SILs from normal epithelium.

Table 4. Association Between Type of p53-Binding Protein 1 (53BP1) Expression and Prognosis of Cervical Intraepithelial Neoplasia.

| | | | Type of 53BP1 Expression at the First Diagnosis, %[a] | | | |
Prognosis	n	Median Observation Period (range), months	Any Type	High DDR	Co-Expression of DDR Types and Ki-67	Ratio of p16[INK4a] Block-Positive Layer (%)[a]
CIN1						
Regressing	11	39 (16-82)	30.6 ± 9.6	12.5 ± 6.7	2.9 ± 2.5	45.6 ± 26.3
Progressing	11	22 (3-41)	31.9 ± 10.6	13.8 ± 9.0	3.0 ± 2.6	41.1 ± 34.0
P value		.013[b]	.77[b]	.81[b]	.92[b]	.78[b]
CIN2						
Regressing	8	16 (6-94)	27.5 ± 15.2	12.2 ± 9.6	3.6 ± 4.4	50.6 ± 26.5
Progressing	13	7 (3-44)	32.5 ± 10.7	13.1 ± 8.2	2.1 ± 2.0	56.8 ± 41.1
P value		.23[b]	.38[b]	.81[b]	0.84[b]	.37[b]

Abbreviations: CIN, cervical intraepithelial neoplasia; DDR, DNA damage response.
[a]Data are shown as mean ± standard deviation.
[b]Mann-Whitney U test.

categorized 22 cases of CIN1 and 21 cases of CIN2 into 2 groups by their prognosis as follows. A total of 24 cases, including 11 cases of CIN1 and 13 cases of CIN2, were categorized as the "progressing" group, having progressed to CIN3 or invasive cancer, whereas the other 19 cases, including 11 cases of CIN1 and 8 cases of CIN2, were categorized as the "regressing group," having regressed to a lower level of CIN or remaining unchanged during the observation period. The observation period of each group is detailed in Table 4. There were no statistically significant associations between CIN prognosis and 53BP1 expression type or the ratio of p16[INK4a] block-positive layer.

Discussion

Uterine cervical SILs frequently affect women in their reproductive years.[24,25] Thus, it is critical to accurately diagnose precancerous lesions and stratify their malignant potential to avoid unnecessary surgical treatment that may increase the risk of miscarriage or premature birth. The current WHO Classification 4th edition defines previous CIN2 and CIN3 as the unified diagnosis of high-grade SIL (HSIL) for improvement in

the diagnostic concordance.[26] However, according to the then diagnostic criteria, the risk of developing cervical cancer of CIN2 and CIN3 was 20% and 40%, respectively. Considering that there was a great difference between their prognoses, clinicians are oftentimes required to decide the clinical management for HSIL, that is, whether to follow-up or perform surgical resection. High-grade SILs—a mixture of CIN2 and CIN3—comprise a heterogeneous group that includes benign and malignant as well as reversible and irreversible lesions. Therefore, finding a new histological indicator that could indicate worse prognosis in SIL cases is critical.

Currently, there are few well-established tools available for SIL diagnosis and management, such as HPV genotyping test and immunohistochemistry for p16[INK4a] expression. We clarified the significance of immunofluorescence analysis of 53BP1 expression as a histologic indicator for cervical carcinogenesis by comparing 53BP1 expression with CIN grade, the type of HR-HPV ISH signals (nonintegrated or integrated), p16[INK4a] expression level, and prognosis by utilizing the SIL cases, for which HR-HPV infection had been confirmed by PCR and a long-term prognosis was completely available. Our results clearly revealed that the number of DDR and abnormal

(co-expression of DDR types and Ki-67) types of 53BP1 expression in cervical tissues was directly proportional to the progression of SIL, integration of HR-HPV shown by ISH analysis, and p16^{INK4a} overexpression. Notably, because the significant difference in type of 53BP1 expression was observed between CIN2 and CIN3, our results indicated the presence of 2 different levels of GIN in HSILs. Further analyses are required to explore the impact of the difference in types of 53BP1 expression among HSILs, which might be helpful to estimate their potential as premalignant lesions. Furthermore, DDR types of 53BP1 expression were detected even in p16^{INK4a}-negative HR-HPV-positive SIL cases, suggesting an early induction of GIN followed by p16^{INK4a} expression in the HR-HPV-infected cervix. Thus, we propose that immunofluorescence analysis of the type of 53BP1 expression can be a useful tool to estimate the GIN in the SIL induced by HR-HPV infection other than the study of p16^{INK4a} expression reflecting replication stress.

We have previously demonstrated that the number of 53BP1 NF in cervical cells increased with progression of cancer.[13] More recently, a similar observation has been reported by Zhu et al.[27] They found that DDR type of 53BP1 NF and low levels of 53BP1 transcript were significantly associated with high histological grade of cervical cancer. Furthermore, low levels of 53BP1 transcript were significantly associated with positive lymph node metastasis of cervical cancer. Thus, because prognostic relevance of 53BP1 expression profile was suggested in cervical cancer,[27,28] we further analyzed the relationships between types of 53BP1 expression and prognosis of CIN1 and CIN2 cases. We found that although DDR types of 53BP1 expression tended to be increased in progressing cases of CIN2, there was no significant association between CIN1 and CIN2 prognosis and 53BP1 expression type as with p16^{INK4a} expression level. Detection of HR-HPV infection has been used to estimate high-risk cases progressing to cancers,[29] and HPV genotyping test is now clinically available for SIL management. Although DDR types of 53BP1 expression can be a surrogate marker for HPV infection and associated with SIL histological grade, 53BP1 expression pattern was not a good predictor of SIL. It is well known that the elimination of HPV by the host immunity dynamically influences SIL outcome, particularly in young women, in which a transient HPV infection can be completely eliminated. We speculate that DDR types of 53BP1 expression might be induced in SIL even by a transient HPV infection that causes GIN but which would be quickly eliminated by host immunity.

The present study had some limitations. First, the sample size was small, which may have led to sampling bias. Secondly, uterine cervical epithelium often reveals various morphological alterations such as metaplasia, inflammation, atrophy, and others. An additional study focused on such benign changes will be necessary.

Diagnosis of SIL is currently based on hematoxylin and eosin staining and auxiliary immunohistochemistry for p16^{INK4a}. Additionally, this study demonstrated that the type of 53BP1 expression was correlated with both SIL grade and p16^{INK4a} expression. We inferred that the integration of HR-HPV into the host genome may be a critical event to induce DDR types of 53BP1 expression in cervical cells. In summary, we propose that 53BP1 expression type can be a valuable biomarker for SIL, which would help estimate the grade and GIN of cervical lesions reflecting replication stress caused by the integration of HR-HPV. Further study is needed to confirm the utility of immunofluorescent analysis of 53BP1 expression as an auxiliary histologic technique to diagnose SIL.

Authors' Note

Acknowledgment

Declaration of Conflicting Interests

Funding

ORCID iD

Sayaka Kawashita https://orcid.org/0000-0002-3635-5300

References

1. Schultz LB, Chehab NH, Malikzay A, Halazonetis TD. P53 binding protein 1 (53BP1) is an early participant in the cellular response to DNA double-strand breaks. *J Cell Biol*. 2000; 151(7):1381-1390.

2. Suzuki K, Yokoyama S, Waseda S, Kodama S, Watanabe M. Delayed reactivation of p53 in the progeny of cells surviving ionizing radiation. *Cancer Res*. 2003;63(5):936-941.

3. Cao L, Xu X, Bunting SF, et al. A selective requirement for 53BP1 in the biological response to genomic instability induced by brca1 deficiency. *Mol. Cell*. 2009;35(4):534-541.

4. Bunting SF, Callén E, Wong N, et al. 53BP1 inhibits homologous recombination in Brca1-deficient cells by blocking resection of DNA breaks. *Cell*. 2010;141(2):243-254.

5. Bouwman P, Aly A, Escandell JM, et al. 53BP1 loss rescues BRCA1 deficiency and is associated with triple-negative and BRCA-mutated breast cancers. *Nat Struct Mol Biol*. 2010;17(6): 688-695.

6. Bunting SF, Callén E, Kozak ML, et al. BRCA1 functions independently of homologous recombination in DNA interstrand crosslink repair. *Mol Cell*. 2012;46(2):125-135.

7. Nakashima M, Suzuki K, Meirmanov S, et al. Foci formation of P53-binding protein 1 in thyroid tumors: Activation of genomic instability during thyroid carcinogenesis. *Int J Cancer*. 2008; 122(5):1082-1088.

8. Naruke Y, Nakashima M, Suzuki K, et al. Alteration of p53-binding protein 1 expression during skin carcinogenesis: Association with genomic instability. *Cancer Sci*. 2008;99(5):946-951.

9. Park JS, Hwang ES, Park SN, et al. Physical status and expression of HPV genes in cervical cancers. *Gynecol Oncol*. 1997;65(1): 121-129.

10. Moody CA, Laimins LA. Human papillomavirus oncoproteins: pathways to transformation. *Nat Rev Cancer*. 2010;10(8): 550-560.

11. Kuner R, Vogt M, Sultmann H, et al. Identification of cellular targets for the human papillomavirus E6 and E7 oncogenes by RNA interference and transcriptome analyses. *J Mol Med (Berl)*. 2007;85(11):1253-1262.

12. Castellsagué X, Schneider A, Kaufmann AM, Bosch FX. HPV vaccination against cervical cancer in women above 25 years of age: key considerations and current perspectives. *Gynecol Oncol*. 2009;115(3 Suppl):S15-S23.

13. Matsuda K, Miura S, Kurashige T, et al. Significance of p53-binding protein 1 nuclear foci in uterine cervical lesions: endogenous DNA double strand breaks and genomic instability during carcinogenesis. *Histopathology*. 2011;59(3):441-451.

14. Tavassoli FA, Devilee P. *Pathology and Genetics of Tumours of the Breast & Female Genital Organs*. Geneva, Switzerland: World Health Organization; 2003.

15. Hopman AH, Kamps MA, Smedts F, Speel EJM, Herrington CS, Ramaekers FCS. HPV in situ hybridization: impact of different protocols on the detection of integrated HPV. *Int J Cancer*. 2005; 115(3):419-428.

16. Omori M, Hashi A, Nakazawa K, et al. Estimation of prognoses for cervical intraepithelial neoplasia 2 by p16[INK4a] immunoexpression and high-risk HPV in situ hybridization signal types. *Am J Clin Pathol*. 2007;128(2):208-217.

17. Cooper K, Herrington CS, Stickland JE, Evans MF, McGee JO. Episomal and integrated human papillomavirus in cervical neoplasia shown by non-isotopic in situ hybridization. *J Clin Pathol*. 1991;44(12):990-996.

18. Konishi I, Fujii S, Nonogaki H, Nanbu Y, Iwai T, Mori T. Immunohistochemical analysis of estrogen receptors, progesterone receptors, Ki-67 antigen, and human papillomavirus DNA in normal and neoplastic epithelium of the uterine cervix. *Cancer*. 1991; 68(6):1340-1350.

19. Al-Saleh W, Delvenne P, Greimers R, Fridman V, Doyen J, Boniver J. Assessment of Ki-67 antigen immunostaining in squamous intraepithelial lesions of the uterine cervix: correlation with the histologic grade and human papillomavirus type. *Am J Clin Pathol*. 1995;104(2):154-160.

20. Dunton CJ, van Hoeven KH, Kovatich AJ, et al. Ki-67 antigen staining as an adjunct to identifying cervical intraepithelial neoplasia. *Gynecol Oncol*. 1997;64(3):451-455.

21. Cuylen S, Blaukopf C, Politi AZ, et al. Ki-67 acts as a biological surfactant to disperse mitotic chromosomes. *Nature*. 2016; 535(7611):308-312.

22. Ishikawa M, Fujii T, Saito M, et al. Overexpression of p16[INK4a] as an indicator for human papillomavirus oncogenic activity in cervical squamous neoplasia. *Int J Gynecol Cancer*. 2006;16(1): 347-353.

23. Vasiljević N, Carter PD, Reuter C, et al. Role of quantitative p16[INK4A] mRNA assay and digital reading of p16[INK4A] immunostained sections in diagnosis of cervical intraepithelial neoplasia. *Int J Cancer*. 2017;141(4):829-836.

24. Fitzmaurice C, Dicker D, Pain A, et al. The global burden of cancer 2013. *JAMA Oncol*. 2015;1(4):505-527.

25. Mezei AK, Armstrong HL, Pedersen HN, et al. Cost-effectiveness of cervical cancer screening methods in low- and middle-income countries: a Systematic review. *Int J Cancer*. 2017;141(3): 437-446.

26. Kurman RJ, Carcangiu ML, Herrington CS, Young RH. *WHO Classification of Tumours of Female Reproductive Organs*. Geneva, Switzerland: World Health Organization; 2014.

27. Zhu H, Yan H, Jin W, et al. The staining patterns of 53BP1 nuclear foci and 53BP1 mRNA level are associated with cervical cancer progression and metastasis. *Int J Gynecol Pathol*. 2014; 33(3):241-247.

28. Roossink F, Wieringa HW, Noordhuis MG, et al. The role of ATM and 53BP1 as predictive markers in cervical cancer. *Int J Cancer*. 2012;131(9):2056-2066.

29. Radley D, Saah A, Stanley M. Persistent infection with human papillomavirus 16 or 18 is strongly linked with high-grade cervical disease. *Hum Vaccin Immunother*. 2016;12(3): 768-772.